Journal Name

COMMUNICATION

Magnetic Conjugated Polymer Nanoparticles Doped with a Europium Complex for Biomedical Imaging

Received 00th January 20xx,
Accepted 00th January 20xx

DOI: 10.1039/x0xx00000x

www.rsc.org/

E. Kemal,[a,b] R. Peters,[a] , S. Bourke,[a] S. Fairclough,[a] P. Bergstrom-Mann,[a] D. M. Owen,[a] L. Sandiford,[a] L. A. Dailey[c]* and M. Green[a]*

Self-assembling conjugated polymer nanoparticles containing PVK and PLGA-PEG as a matrix polymer were doped with both a luminescent rare-earth complex and magnetic nanoparticles (SPIONs), giving rise to materials that are both luminescent and magnetic. Nanoparticle sizes ranged from 80 - 110 nm without SPIONs and showed an increase in size (200 - 1000 nm) with additional SPION content (11-54%). Quantum yields (QYs) of 24% and 18% were measured for systems without and with 11% SPIONs, respectively. Optical properties were stable and suitable for biological imaging applications.

Π-conjugated polymers are of interest for a wide range of applications in fluorescence imaging and drug delivery. Compared to fluorescent dyes and quantum dots, π-conjugated polymers possess larger absorption cross-sections, brighter emission, and high photostability.[1-5] In contrast, rare-earth ions have very narrow emission spectra and it has been previously documented that rare-earth complexes containing β-diketonate ligands, such as tris(dibenzoylmethane)mono(1,10-phenanthroline) (III) ($Eu(dbm)_3phen$), display long luminescence lifetimes, high colour purity, and intense emission.[6] This emission can be excited through Förster transfer by doping $Eu(dbm)_3phen$ complexes into nanoparticles containing a blue emitting conjugated polymer, such as poly(9-vinylcarbazole) (PVK).[6,7] Physically, the π-conjugated polymer, PVK, functions as a hydrophobic matrix into which the lipophilic europium complex is dispersed, in addition to acting as an efficient fluorescence energy donor.

The introduction of further components into the NPs can be used to further enhance the system for bimodal imaging, such as addition of SPIONs for MRI imaging. For example, Howes *et al*.[8] reported the preparation of π-conjugated polymer nanoparticles (CPNs) comprised of four different π-conjugated polymers containing 20% (w/w%) superparamagnetic iron oxide nanoparticles (SPIONs). To achieve colloidal stability, the CPNs were stabilised by polyethylene glycol (PEG) conjugated-phospholipids. The bimodal CPNs produced thus ranged in size (150 – 400 nm), exhibited QY values between 0.4-2.2% and were shown to have a shortening effect on the transverse T2* relaxation time. A further advantage included material manipulation through use of a simple bar magnet, providing an extremely simple method of CPN purification.[8]

Disadvantages associated with the use of pegylated phospholipids for the colloidal stabilisation of CPN include both the high cost of these materials, as well as their displacement from the particle surface when introduced into biological fluids.[9,10] We have explored other capping agents, such as amphiphilic proteins.[11] However, pegylation of the CPN surface is useful, as it prolongs the circulation lifetime of materials *in vivo* due to decreased recognition and clearance from the body by the mononuclear phagocytic system[12,13]. To avoid loss of pegylated surfactant from the CPN surface through biomolecule displacement, an alternative approach using amphiphilic co-polymers as matrix forming agents has been tested with some success.[14,15] For example, Abelha *et al*.[14] and Kemal *et al*.[15] have both reported that different π-conjugated polymers can be embedded within self-assembling polymer micelles comprised of the copolymer of polylactic-*co*-glycolic-polyethylene glycol (PLGA-PEG) at extremely high production yields. The resulting CPNs are typically 140-160 nm in size and have high QYs (30-40%) depending on the type of π-conjugated polymer used. Since PLGA is a family of FDA-approved biodegradable polymers and PLGA-PEG copolymers have been extensively studied as delivery vehicles for drugs, proteins and various other macromolecules such as DNA, RNA, and peptides, it has favourable properties as a matrix material for injectable contrast agents. [16]

Inspired by previous work[8,17-21] we report a strategy in which $Eu(dbm)_3phen$ was doped into CPNs comprising of PLGA-PEG

[a] Department of Physics, King's College London, Strand, London, WC2R 2LS.
[b] Department of Pharmacy & Forensic Science, King's College London, Fifth Floor, Franklin-Wilkins Building, Waterloo Campus, London, SE1 9NH.
[c] Department of Pharmacy, Martin-Luther-Universität Halle-Wittenberg, Wolfgang-Langenbeck-Str. 4, 06120 Halle (Saale), Germany
Electronic Supplementary Information (ESI) available: Experimental procedures, movie of magnetic nanoparticles and characterisation of particles.
See DOI: 10.1039/x0xx00000x

and PVK. Single crystal domain SPIONs were then incorporated into the systems (11-54% w/w%) and their physicochemical and optical properties assessed. It was hypothesised that the PLGA-PEG would shield and effectively protect the hydrophobic polymer in the CPN core. To optimise system properties, two parameters were investigated: the PLGA-PEG molecular weight (6, 17 or 60 kDa) and PLGA-PEG mass ratio (63% vs 89%) (Table 1). Nanoparticles prepared with 63% PLGA-PEG exhibited hydrodynamic diameters between 150 - 190 nm, while an increase in the PLGA-PEG content to 89% resulted in a slightly narrower size range (145 - 165 nm) as assessed by dynamic light scattering (DLS).

PLGA-PEG MW	*Mass ratio PLGA-PEG : PVK : Eu(dbm)$_3$phen*	Hydrodynamic diameter/ nm ± SD	Polydispersity index ± SD
6 kDa	**63**:31:6	149.4 ± 2.5	0.2 ± 0.0
	89:9:2	163.4 ± 4.2	0.2 ± 0.0
17 kDa	**63**:31:6	164.4 ± 3.4	0.2 ± 0.0
	89:9:2	145.3 ± 3.3	0.1 ± 0.1
60 kDa	**63**:31:6	188.1 ± 3.4	0.3 ± 0.1
	89:9:2	154.0 ± 3.4	0.20 ± 0.1

Table 1. Hydrodynamic diameters (nm) of nanoparticles with varying PEG-PLGA content and molecular weight. Values represent the mean ± standard deviation of n=4 measurements.

The molecular weight of the PLGA-PEG also had an impact on PVK photoluminescence (PL), whereby the 6 kDa PLGA-PEG quenched PVK PL, while the larger molecular weight PLGA-PEG polymers did not (supporting information figure 1). Based on this finding, all further systems were prepared using 63% of 60 kDa PLGA-PEG (with 31% PVK and 6% Eu(dbm)$_3$phen). To investigate the impact of SPION incorporation on the particle size, CPNs were prepared containing 11-54% (w/w%) SPIONS. Based on this observation, systems with 11% SPIONs alone were further characterised.

TEM images of the magnetic CPNs showed that particles were approximately spherical with the inorganic particles clearly visible as dark spheres unevenly distributed within the body of the nanoparticle assembly (figure 1). The multimodal nanoparticles responded to a bar magnet whilst retaining the bright emissive properties under 365 nm excitation (movie for particles containing 11% iron oxide, supporting information).

A superconducting quantum interference device (SQUID) magnetometer was used to characterise the magnetic behaviour of the CPNs. They were analysed by drawing their M-H loops in an applied field ranging from -14kOe to 14kOe at 310K (36.5°C) (Supporting information figure 2). The M-H curve of the CPN exhibits saturation of magnetisation (emu/g) up to 1.5 emu g^{-1}. While this value is low, the small amount of SPIONs added plus the density of the CPN does suggest superparamagnetic properties (further confirmed by the net magnetization of the particle assemblies in the absence of an external field was zero). Typical absorption and emission profiles of PVK, Eu(dbm)$_3$phen, and CPN with 11% SPIONs are depicted in Figure 2A. PVK alone displayed broad emission between 400 - 500 nm (excitation: 365 nm), whilst the

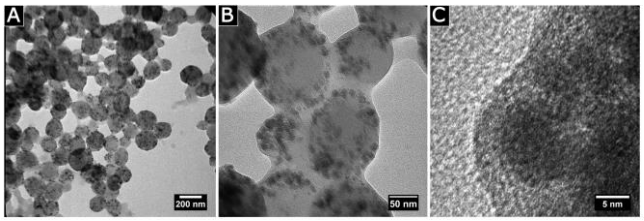

Figure 1. TEM images of CPNs with SPIONs at 63% of P60K PLGA-PEG. (A) shows wide view of NPs with an average size of 150 nm, (scale bar = 200 nm) (B) is a higher magnification in order to highlight the iron oxide SPIONs (black dots) contained within the NP (scale bar = 50 nm). C) High resolution image of the SPIONs (scale bar = 5 nm).

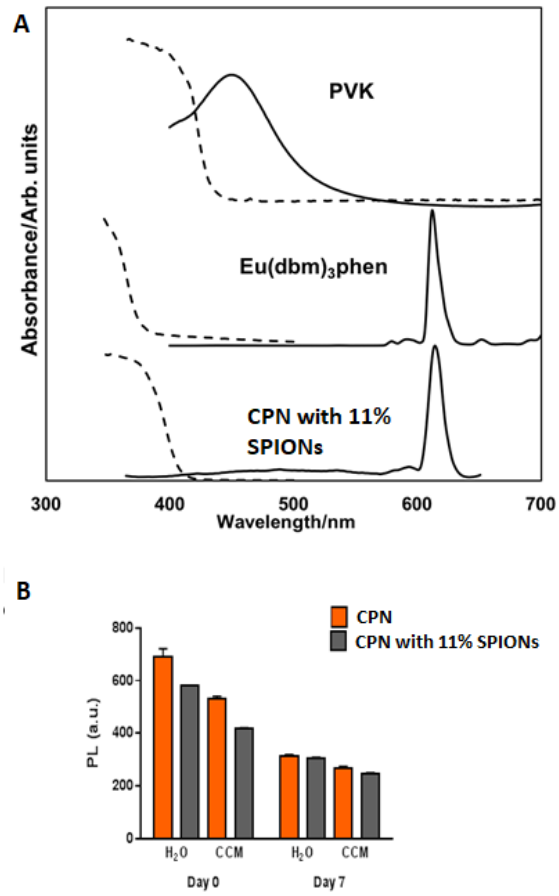

Figure 2. A) Normalised absorption and emission profiles of PVK and Eu(dbm)$_3$phen in solution, compared with optimised CPN containing 11% SPIONs. (B) Fluorescence intensity (arbitrary units) of CPN with and without 11% SPIONs in purified water and serum-supplemented cell culture medium. Values represent the mean ± standard deviation of n=3 replicate batches of nanoparticles.

Eu(dbm)$_3$phen exhibited a narrow peak at *ca.* 612 nm. The CPNs containing 11% SPIONs had an emission spectrum matching the Eu(dbm)$_3$phen complex, indicating successful energy transfer. The absolute QY of CPNs with 0% and 11% SPIONs was 24% and 18%, respectively.

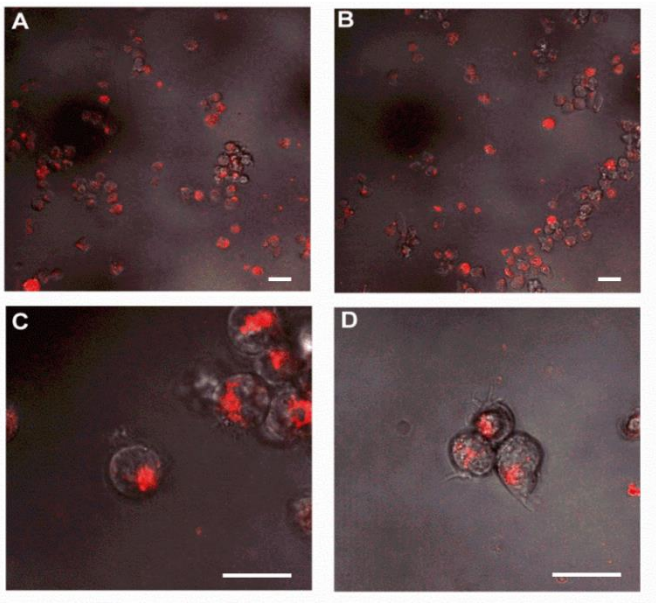

Figure 3. Overlaid confocal images (Brightfield/570 - 620 nm channel) of the CPNs without (A, B) and with 11% SPIONS (C, D) following 1 h incubation with isolated human T cells respectively. Scale bar = 5 µm.

In preparation for cell culture studies, the PL intensity of CPNs with and without 11% SPIONs was measured over a 7-day period in both water and cell media(CCM) supplemented with 10% foetal bovine serum (FBS) at 37°C + 5% CO_2 (Figure 2B). It was observed that the presence of SPIONs in the nanoparticles reduced the PL by *ca*. 15% and measurement in CCM also showed a decreased PL. In all cases, the CPN emission was reduced significantly over 7 days ($P<0.05$) which we assign to water quenching lanthanide emission. To investigate their potential use as bio-imaging agents, laser scanning confocal microscopy (LSCM) was performed. The association of CPNs with and without 11% SPIONs with isolated primary human T lymphocytes was demonstrated (Figure 3). Despite a PEG coating, which has been previously shown to minimise cell surface interactions, the nanoparticles appeared to directly associate with the primary T cells.

SPION incorporation into polymeric nanoparticles has been shown to increase the particle size as reported here and in previous studies[8,22]. In a similar strategy, Talleli *et al*[22] utilised self-assembling copolymers of PEG-b-poly[N-(2-hydroxypropyl) methacrylamide dilactate] to encapsulate up to 40% SPIONs with a size increase from 150 - 350 nm depending on the SPION content. When comparing this to the results in this study, it is assumed that simultaneous incorporation of the PVK and SPIONs contributes to larger size increases than SPIONs alone.

In comparison to previous work, the CPNs with 11% SPIONs produced in this study exhibited considerably high QYs (18%) compared to CPN containing 20% SPIONs reported by Howes *et al* (0.4-2.2%).[8] This may be attributed both to the comparatively lower amount of SPIONs used in the current study, but also to a different spatial organisation of the SPIONs within the nanoparticle structure. Ongoing studies are investigating the impact of the SPION organisation on the optimised CPN properties. Further studies also include assessment of particle stability and biodegradation rate in biological media, cell compatibility studies and surface modification.

In conclusion, we have prepared magnetic red-emitting conjugated polymer particles by doping an rare earth complex and magnetic iron oxide nanoparticles into a self-assembling PVK:PLGA-PEG matrix. The resulting nanomaterials had excellent optical properties and could be used in cell imaging experiments, which highlights the potential of this system.

Acknowledgements

We acknowledge EPSRC for funding (EP/K018876/1).

References

1 J. Pecher and S. Mecking, *Chem. Rev.* 2010, **110**, 6260.
2 A. Kaeser and A. P. H. Schenning, *J. Adv. Mater.* 2010, **22**, 2985.
3 D. Tuncel and H. V. Demir, *Nanoscale*, 2010, **2**, 484.
4 C. Wu and D. T. Chiu, *Angew. Chem. Int. Ed.* 2013, **52**, 3086.
5 C.-P. Chen, P.-J. Wu, S.-Y. Liou and Y.-H. Chan, *RSC Adv.* 2013, **3**, 17507.
6 M. D. McGeeHee, T. Bergstedt, C. Zhang, A. P. Saab, M. B. O'Regan, G. C. Bazan, V. I. Srdanov and A. J. Heeger, *Adv. Mater.* 1999, **11**, 1349.
7 J. Yu, R. Deng, Y. Rong, B. Fujimoto, C. Wu, H. Zhang and D. T. Chiu, *Angew. Chem. Int. Ed,* 2013, **52**, 11294.
8 P. Howes, M. Green, A. Bowers, D. Parker, G. Varma, M. Kallumadil, M. Hughes and A. Warley, *J. Am. Chem. Soc.* 2010, **132**, 9833.
9 R. Ahmad Khanbeigi, T. F. Abelha, A. Woods, O. Rastoin, R. D. Harvey, M. C. Jones, B. Forbes, M. A. Green, H. Collins and L.-A. Dailey, *Biomacromol.* 2015, **16**, 733.
10 R.A. Khanbeigi, Z. Hashim, T.F. Abelha, S. Pitchford, H. Collins, M.A. Green, L.A. Dailey. *J Mater Chem B,* 2015, **3** 2463.
11 R. Peters, L. Sandiford, D. M. Owen, E. Kemal, L. A. Dailey, M. Green, Photochem. Photobiol. Sci, 2016, 15, 1448.
12 D. Zhang, M. Wu, Y. Zeng, N. Liao, Z. Cai, G. Liu, X. Liu and J. Liu, *J. Mater. Chem. B.* 2016, **4**, 589.
13 J. V. Jokerst, T. Lobovkina, R. N. Zare and S. S. Gambhir, *Nanomedicine (Lond).* 2011, **6**, 715.
14 T.F. Abelha, T.W., Phillips, J.H. Bannock, A.M. Nightingale, C.A. Dreiss, E. Kemal, L. Urbano, J.C. DeMello, M.A. Green, L.A. Dailey. *Nanoscale,* 2017, **9**, 2009.
15 E., Kemal, T.F. Abelha, L. Urbano, R. Peters, D.M. Owen, P. Howes, M.A. Green, L.A Dailey. *RSC Advances*, 2017, **7**, 15255.
16 J. Cheng, B. A. Teply, I. Sherifi, J. Sung, G. Luther, F. X. Gu, E. Levy-Nissenbaum, A. F. Radovic-Moreno, R. Langer and O. C. Farokhza, *Biomaterials*, 2007, **28**, 869.
17 F. Ye, C. C. White, Y. Jin, X. Hu, S. Hayden, X. Zhang, X. Gao, T. J. Kavanagh and D. T. Chiu, *Nanoscale*, 2015, **7**, 10085.
18 A. Das and P. T. Snee, *ChemPhysChem*, 2016, **17**, 598.
19 M. D. McGehee, T. Bergstedt, C. Zhang, A. P. Saab, M. B. O'Regan, G. C. Bazan, V. I. Srdanov and A. J. Heeger, *Adv. Mater.* 1999, **11**, 1349.

20 Q. Li, J. Zhang, W. Sun, J. Yu, C. Wu, W. Qin and D. T. Chiu, *Langmuir*, 2014, **30**, 8607.
21 W. Sun, J. Yu, R. Deng, Y. Rong, B. Fujimoto, C. Wu, H. Zhang and D. T. Chiu, *Angew. Chem. Int. Ed.* 2013, **52**, 11294.
22 M. Talelli, C. J. F. Rijcken, T. Lammers, P.R. Seevinck, G. Storm, C. F. van Nostrum, W. E. Hennink, *Langmuir,* 2009, **25**, 2060.

